J Sol-Gel Sci Technol (2009) 49:209–220
DOI 10.1007/s10971-008-1861-6

ORIGINAL PAPER

Polyurea based aerogel for a high performance thermal insulation material

Je Kyun Lee · George L. Gould · Wendell Rhine

Received: 28 June 2008 / Accepted: 12 November 2008 / Published online: 4 December 2008

Abstract Less fragile lightweight nanostructured polyurea based organic aerogels were prepared via a simple sol–gel processing and supercritical drying method. The uniform polyurea wet gels were first prepared at room temperature and atmospheric pressure by reacting different isocyanates with polyamines using a tertiary amine (triethylamine) catalyst. Gelation kinetics, uniformity of wet gel, and properties of aerogel products were significantly affected by both target density (i.e., solid content) and equivalent weight (EW) ratio of the isocyanate resin and polyamine hardener. A supercritical carbon dioxide (CO_2) drying method was used to extract solvent from wet polyurea gels to afford nanoporous aerogels. The thermal conductivity values of polyurea based aerogel were measured at pressures from ambient to 0.075 torr and at temperatures from room temperature to −120 °C under a pressure of 8 torr. The polyurea based aerogel samples demonstrated high porosities, low thermal conductivity values, hydrophobicity properties, relatively high thermal decomposition temperature (~270 °C) and low degassing property and were less dusty than silica aerogels. We found that the low thermal conductivities of polyurea based aerogels were associated with their small pore sizes. These polyurea based aerogels are very promising candidates for cryogenic insulation applications and as a thermal insulation component of spacesuits.

J. K. Lee (✉) · G. L. Gould · W. Rhine
Research and Development Division, Aspen Aerogels, Inc,
30 Forbes Road, Building B, Northborough, MA 01532, USA
e-mail: jekyun@aerogel.com

G. L. Gould
e-mail: ggould@aerogel.com

W. Rhine
e-mail: wrhine@aerogel.com

Keywords Polyurea · Aerogels · Thermal conductivity · Supercritical drying · Nanoporous · Insulation

1 Introduction

Nanoporous materials can be produced by replacing the liquid solvent phase within the nanometer-sized pores with air without collapsing the pore structure. As shown in Eq. 1, the capillary pressure is inversely related to the pore size. For materials with nanometer pore sizes, the capillary pressure is high; and therefore, the tendency toward pore collapse during solvent evaporation is overwhelming and materials will shrink when dried at ambient pressures and temperatures:

$$P_c = 2\gamma_{L-V}\cos\theta/r_p \quad (1)$$

where, P_c = capillary pressure, γ_{L-V} = interfacial tension (liquid vapor interface), θ = solvent-surface contact angle, and r_p = pore radius (or radius of curvature).

Kistler [1, 2] produced the first aerogels from a silica gel by replacing the liquid phase with air and demonstrated that the gel's pore structure was maintained by drying the gels under supercritical conditions where the interfacial tension (γ_{L-V}) between liquid and the vapor phase is reduced to near zero; and thus, the strong capillary forces that cause shrinkage and pore collapse are eliminated. Based on his investigation, aerogel materials are typically prepared by removing the solvent contained in a gel matrix by extraction in a supercritical fluid medium after bringing the gel solvent system above its critical temperature and pressure and subsequently relieving pressure above the critical temperature until only vapor remains. One popular extraction solvent is carbon dioxide because it is inexpensive and has a relatively low critical temperature (31 °C) and critical pressure

(7.3 MPa) [3–6]. Alternatively, the gel solvent system can be extracted by contacting the wet gel with an appropriate solvent.

The general preparation methods, the unique physical and thermal properties, and future potential applications of aerogels can be found in several outstanding review papers [3–7]. Silica aerogels prepared via sol–gel processing and supercritical drying can exhibit extremely low density, high surface area, and attractive optical, dielectric, thermal, and acoustic properties [8, 9]. These excellent properties explain why aerogels have been considered for use in thermal and acoustic insulation applications [3–7, 10–12].

Although silica aerogels demonstrate many unusual and useful properties, commercialization has been limited because of their low strength, brittleness, and (to date) high production costs. There are several strategies to overcoming the drawbacks associated with the weakness and brittleness of silica aerogels. Flexible fiber reinforced silica aerogel composite blankets have been developed and proven to be a significant breakthrough in producing advanced thermal insulation materials for use at low and high temperatures [13]. Although the fiber reinforcement significantly improved the properties of silica aerogel blankets, they are still dusty due to the inherent brittleness of silica aerogels. Further reducing the aerogel blankets dustiness and increasing their durability would significantly expand the potential applications for aerogel insulation materials.

Nanoporous aerogel materials have also been derived from organic polymers, some of which can be converted to carbon aerogels. Pekala and co-workers [14–21] have intensively studied organic aerogels related to resorcinol/formaldehyde (RF), melamine/formaldehyde (MF), and phenolic/furfural (PF). These RF, MF, and PF organic aerogels can be converted into carbon aerogels by pyrolysis. On the other hand, Tan et al. [22] reported cellulose aerogels with significantly improved impact strength, while Fischer et al. [23] recently investigated an alternate cellulose aerogel that incorporated a non-toxic polyisocyanate cross-linking agent. These organic aerogels were stronger than silica aerogels showing very high impact strengths. However, these organic aerogels are also too brittle, rigid, and/or dusty to be used for some insulation applications.

Polyisocyanurate based organic aerogels were prepared by drying at ambient or supercritical conditions and the corresponding carbon aerogels were prepared by pyrolysis of the organic aerogels under an inert atmosphere [24–26]. Biesmans et al. produced their organic aerogels by a conventional CO_2 supercritical drying process, after preparing polyisocyanurate wet gel by trimerization reaction of isocyanate with catalyst at different temperatures. Although the polyisocyanurate aerogels were prepared with a wide range of densities, high surface areas and small pore sizes, and reasonably good thermal conductivity property, they shrank during supercritical drying mainly due to trimerization reaction of isocyanate. Also, the polyisocyanurate aerogels were generally brittle and dusty [26]. Polyurethane (PU) based xerogels and aerogels were recently studied using different isocyanates and polyol hardeners by drying at ambient or supercritical condition [26, 27]. Although the aerogels demonstrated good thermal conductivity values at low pressures, they showed higher thermal conductivity values at ambient pressures, and these thermal conductivities need to be reduced before they can be useful for thermal insulation applications.

Contrary to these many previous inorganic and organic aerogel studies, little work has been devoted to developing polyurea based aerogels and understanding the basic relationship between material variables and properties of the polyurea based aerogels. The molecular structure of a typical polyurea consists of alternating hard and aromatic isocyanate segments and soft polyamine chains (generally, polydiamines or polytriamines containing terminal hydroxyl ($–NH_2$) groups) and are similar to PU molecular structures.

Figure 1 illustrates the typical PU and polyurea structure formed from the reaction of an isocyanate with a diol or a diamine. Also, similar to the PU system, a wide range of different properties can be obtained by designing polyurea molecular structures. The reaction between isocyanates and amines is generally faster than the reaction between isocyanates and alcohols, which is a great advantage in the production of aerogel materials using sol–gel processing. The primary objective of this study is to investigate the feasibility of preparing lightweight, nanostructured polyurea based aerogels suitable for a high performance insulation material.

2 Experimental

Commercially available methylene diphenyl diisocyanate (MDI), polymeric methane diphenyl diisocyanate (pMDI), polyamine and polyol hardeners, catalyst, and solvents were used for preparing polyurea and PU based aerogel samples.

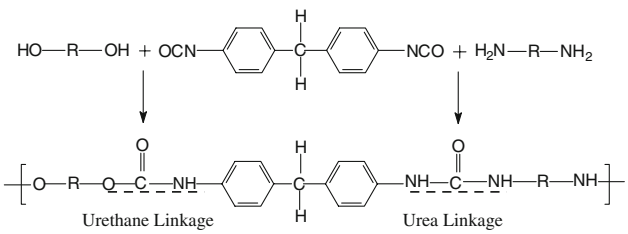

Fig. 1 Formation of polyurethane and polyurea structures from the reaction between an isocyanate and a diol or a diamine, respectively

MDI (Mondur ML for polyurea 1) and pMDI (PAPI 94 for polyurea 2) were obtained from Bayer Corporation and Dow Chemical, respectively, and polyoxypropylene triamines available as Jeffamine-T3000 (polyamine 1) and T5000 (polyamine 2) with molecular weights (M_w) of approximately 3000 and 5000 g/mol obtained from Huntsman LLC were used as polyamine hardeners. Polyether polyol modified with ethylene oxide (Multranol 9185) with relatively high M_w was used as a polyol hardener for preparing PU aerogels, while MDI was used as a matrix resin for preparing PU aerogels. The reagent grade triethylamine (TEA) used as a catalyst for preparing both polyurea and PU aerogels was purchased from Aldrich. Acetone was mostly used for the aging solvent due to relatively easy solvent exchange with CO_2 during supercritical drying as well as for the gelation solvent due to the uniform wet gel formation, unless otherwise noted. All materials were used as received without further purification. All formulations were gelled at ambient conditions and aged at 50 °C for 2 days, unless otherwise noted. The sample preparation procedure for polyurea (or PU) based aerogels is illustrated in Fig. 2.

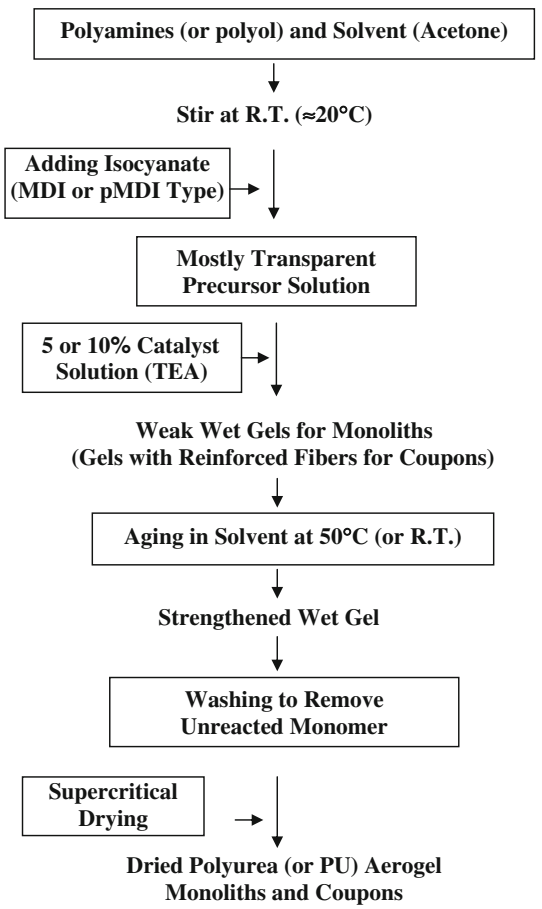

Fig. 2 Flow chart for the preparation procedure of polyurea (or PU) based aerogel monolith and coupon samples

Basic properties of the gel systems such as gel time, bulk density, shrinkage factor, thermal conductivity at different pressures and temperatures including atmospheric conditions, and pore volume and pore size distribution, and thermal decomposition temperatures were measured. Gel time was defined as the time following addition of all the catalyst into the sol, to the gelation point of the sol which is defined as when the sample did not move with gentle shaking. The shrinkage factor is defined as the ratio of the final density of the dried samples to the target density calculated from solid content in the sol: Shrinkage Factor (f) = Final Density (g/cm^3)/Target Density (g/cm^3). Also, assuming polyurea has a density of 1.20 g/cc based on the densities and weight ratio of isocyanate and polyamine, the total porosity (%) was calculated: porosity (%) = 100 − [[bulk polyurea aerogel density (g/cm^3)/1.20 g/cm^3] × 100]. Thermal conductivity at a single mean temperature of 37.8 °C was measured using a custom heat flow meter that consists of a hot plate, a NIST-calibrated reference sample (i.e., polystyrene), aerogel sample for measurement, and thermocouples, which was schematically illustrated in [28]. Thermal conductivity (λ) values at different pressures and temperatures were calculated using Eq. 2 [29]:

$$\lambda = \alpha \cdot C_p \cdot \rho \quad (2)$$

where thermal diffusivity values (α) were measured using the step heat method [30], specific heat (C_p) values were determined using a differential scanning calorimeter, and bulk density (ρ) values were calculated from sample geometries and masses.

The BET surface area, pore volume, average pore size, and pore size distribution were measured by using liquid nitrogen absorption method in Accelerated Surface Area and Porosimetry Measurement System (Micromeritics Instrument Co., Model: ASAP 2010) after degassing at 70 °C (105 °C for silica aerogel) for 12 h. Microstructures were measured by using a field-emission scanning electron microscope (FESEM, JEOL JSM-6335F). The fracture surface of each sample was used for FESEM measurements [28]. The thermal stability, decomposition temperature, and mass loss were measured by using TG-DTA/DSC (Netzsch Instruments, Inc. Model: STA 449C Jupiter).

The effect of the ratio of amine hydrogen equivalent weight to isocyanate equivalent weight (EW ratio (equivalent weight of NH/equivalent weight of NCO)) on the shrinkage factor and thermal conductivity values of the polyurea based aerogel monoliths prepared with a constant target density of 0.1 g/cm^3 and a catalyst content of 5 wt% was first studied as functions of two isocyanate and polytriamine types. Table 1 lists the isocyanate, polyamine and EW ratio used to prepare the samples for the experiments. It is generally known that an equivalent weight (EW) ratio

Table 1 Recipes used to prepare the aerogels to study the effect of the ratio of amine hydrogen equivalent weight to isocyanate equivalent weight (EW ratio) on the shrinkage factor and thermal conductivity values of the polyurea based aerogels

Sample No.	Isocyanates	Polyamines[a]	EW Ratio (wt/wt)
Polyurea 1-A1	MDI	Polyamine 1	0.1
Polyurea 1-A2	MDI	Polyamine 1	0.3
Polyurea 1-A3	MDI	Polyamine 1	0.5
Polyurea 1-A4	MDI	Polyamine 1	0.7
Polyurea 2-A5	pMDI	Polyamine 1	0.1
Polyurea 2-A6	pMDI	Polyamine 1	0.3
Polyurea 2-A7	pMDI	Polyamine 1	0.5
Polyurea 2-A8	pMDI	Polyamine 1	0.7
Polyurea 3-A9	MDI	Polyamine 2	0.1
Polyurea 3-A10	MDI	Polyamine 2	0.3
Polyurea 3-A11	MDI	Polyamine 2	0.5
Polyurea 3-A12	MDI	Polyamine 2	0.7
Polyurea 4-A13	pMDI	Polyamine 2	0.1
Polyurea 4-A14	pMDI	Polyamine 2	0.3
Polyurea 4-A15	pMDI	Polyamine 2	0.5
Polyurea 4-A16	pMDI	Polyamine 2	0.7

[a] See Sect. 2 for more details

of approximately 1 may provide the best physical properties for bulk polyurea and PU systems.

The effect of target density on the properties of polyurea 2 aerogels prepared with an EW ratio (NH/NCO) of 0.1 and with 5 and 10 wt% catalyst contents were studied. Table 2 provides the target densities and EW ratios used to prepare the polyurea 2 aerogels. Some of these samples were chosen to investigate the microstructure of the aerogels by SEM. Also, in order to find the optimum values of target density and EW ratio, we conducted a 2 variable, 3 level, 9 sample full factorial DOE experiment. Table 3 summarizes the material variables and levels used to prepare the samples for the DOE experiment. The objective of the DOE method used in this study was to quantitatively analyze the

Table 2 Recipe used to prepare the aerogels to study the effect of target density on important properties of polyurea 2 based aerogels prepared with 5 and 10 wt% catalyst content

Exp. No.	Factor 1 ρ_{Target} (g/cm^3)	EW ratio (wt/wt)
Exp-1	0.05	0.1
Exp-2[a]	0.06	0.1
Exp-3	0.08	0.1
Exp-4[a]	0.1	0.1
Exp-5	0.12	0.1
Exp-6	0.15	0.1
Exp-7	0.2	0.1

[a] Also used for the microstructure study

Table 3 Material variables and levels used for a 3-level, 2-factor, 9 experiment full factorial DOE method conducted at catalyst contents of 5 and 10 wt%

Exp. No.	Factor 1 ρ_{Target} (g/cm^3)	Factor 2 EW Ratio (wt/wt)
DOE-1	0.06	0.05
DOE-2	0.06	0.10
DOE-3	0.06	0.15
DOE-4	0.08	0.05
DOE-5	0.08	0.10
DOE-6	0.08	0.15
DOE-7	0.10	0.05
DOE-8	0.10	0.10
DOE-9	0.10	0.15

effects of these material variables on the properties of the polyurea based aerogels. Statisca™ (StatSoft®) DOE software was used for experimental design and data analysis.

3 Results and discussion

Figure 3 illustrates shrinkage factors of polyurea aerogel monoliths prepared with different isocyanates and polyamine hardeners at a constant target density of 0.1 g/cm^3 and a catalyst content of 5 wt% as a function of EW ratio. Figure 3 shows that as higher EW ratios are used, higher shrinkage factors are observed for the polyurea based aerogel monolith samples after supercritical drying. More uniformly and densely cross-linked polyurea wet gel structure resulting from higher isocyanates content (i.e., smaller EW ratio (NH/NCO)) may be associated with less

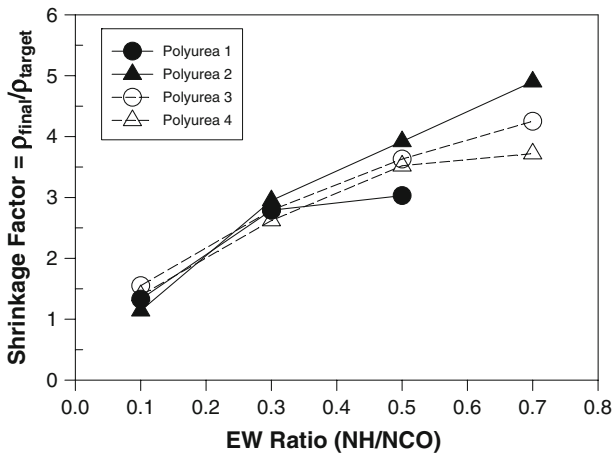

Fig. 3 Shrinkage factors of polyurea based aerogel monoliths prepared with a recipe shown in Table 1 and a constant target density of 0.1 g/cm^3 and a catalyst content of 5 wt% as a function of EW ratio

Table 4 Shrinkage factor and thermal conductivity values measured for the polyurea based aerogel samples prepared using the recipe of Table 1

Sample	Shrinkage factor	Thermal conductivity value (mW/m K)[a]
Polyurea 1-A1	1.33	18.2 ± 1.12
Polyurea 1-A2	2.79	25.3 ± 0.68
Polyurea 2-A5	1.14	19.2 ± 1.35
Polyurea 2-A6	2.95	28.5 ± 2.84
Polyurea 3-A9	1.55	29.5 ± 1.04
Polyurea 3-A10	2.79	36.3 ± 2.16
Polyurea 4-A13	1.39	26.7 ± 1.67
Polyurea 4-A14	2.62	35.6 ± 2.76

[a] Average of 5 thicknesses measured at five different places was used. Measurements were conducted at 37.8 °C under compression of about 0.1 psi

shrinkage during aging and supercritical drying. Overall, the polyurea aerogel samples prepared with excess isocyanate exhibited little shrinkage and remained monolithic which is consistent with previous results observed from PU aerogels [26, 27].

Table 4 provides shrinkage factor and thermal conductivity values measured from the polyurea based aerogel monoliths with good appearances prepared with EW ratio of 0.1 and 0.3 and a target density of 0.1 g/cm^3. Polyurea 1 and 2 based aerogel monoliths prepared with polyamine 1 generally show smaller shrinkage factors, lower thermal conductivity values, and less dustiness than those prepared with polyamine 2, while polyurea 3 and 4 based aerogels prepared with polyamines 2 were more flexible.

Based on these results, polyamine 1 was selected as a main polyamine hardener and used for the rest of this study. Note that polyamine 1 and 2 have the same molecular structure, although polyamine 1 (T3000) has a lower M_w. Faster reactions and higher crosslinked structures formed by the reaction of isocyanates and polyamine 1 at a low EW ratio of 0.1 may be considered as main reasons for lower shrinkage and lower thermal conductivity values than those formed by isocyanates and polyamine 2. On the other hand, polyurea 2 based samples prepared with pMDI generally were more flexible and less dusty than the polyurea 1 based aerogel samples prepared with MDI.

To better understand the effects of the hardener and EW ratio on shrinkage factors of the aerogel samples, we prepared polyurea 1 and PU based aerogel samples using two different EW ratios. Figure 4 shows photos of the polyurea 1 and PU aerogel monoliths and fiber reinforced coupons prepared with EW ratio of 0.1 and 0.15 and a constant target density of 0.1 g/cc and TEA catalyst content of 5 wt%. As shown in Fig. 4, polyurea aerogel monoliths and coupons are generally larger than PU aerogel samples

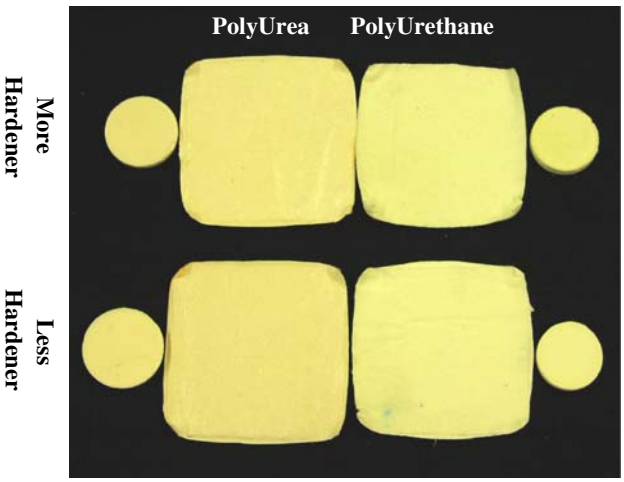

Fig. 4 Photographs of polyurea and PU based aerogel monoliths and coupons produced with two EW ratios (NH or OH/NCO) of 0.1 and 0.15 and a constant target density of 0.1 g/cm^3 and a catalyst content of 5 wt%

indicating less shrinkage. Figure 4 also shows that both polyurea and PU aerogel monoliths and coupons prepared with less hardener content (i.e., smaller EW ratio (NH or OH/NCO)) show less shrinkage than observed for samples prepared with higher hardener content implying that polyurea and PU wet gel with higher crosslink densities shrink less during drying. The coupon samples are currently being used to investigate the relationship among material variables, thermal conductivities, and mechanical properties. The results for the coupons will be separately reported in a future paper.

The gelation time of polyurea 2 prepared with a constant EW ratio of 0.1 and 5 and 10 wt% catalyst contents was studied as a function of the target density, and the results are given in Fig. 5. Note that during gelation there was a phase transition from the transparent light yellow urea

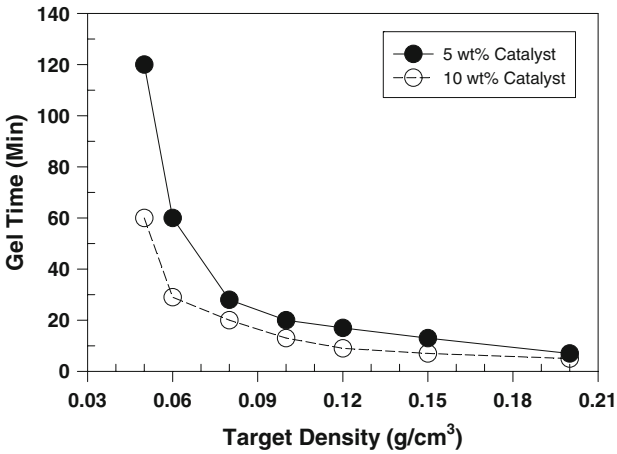

Fig. 5 The relationship between the gel times and the target densities and catalyst concentration for polyurea 2

solution to an opaque polyurea wet gel, which is a result of light scattering by the polymerized polyurea gel. Figure 5 shows that faster gel formation times occur with increasing target density (i.e., solid content) and catalyst content. However, the effect of catalyst content on the polyurea gel formation was less significant than it was for other aerogel systems such as polydicyclopentadiene (pDCPD) [28] and silica aerogels [31] previously reported.

Figure 6 illustrates the effect of target density and final density on the shrinkage factor and thermal conductivity values of the polyurea based aerogels, respectively, prepared with a constant EW ratio of 0.1 and a catalyst content of 5 wt%. The data presented in Fig. 6 indicates that both shrinkage factors and thermal conductivity values (determined at 37.8 °C) of the polyurea based aerogels decrease with increasing target and final density, respectively, until they reach the minimum values. After they reach the minimum value, they increase with further increasing target and final density. Since shrinkage during aging and supercritical drying generally affect their final densities, it is reasonable to observe a close relationship between the shrinkage factor, density and thermal conductivity.

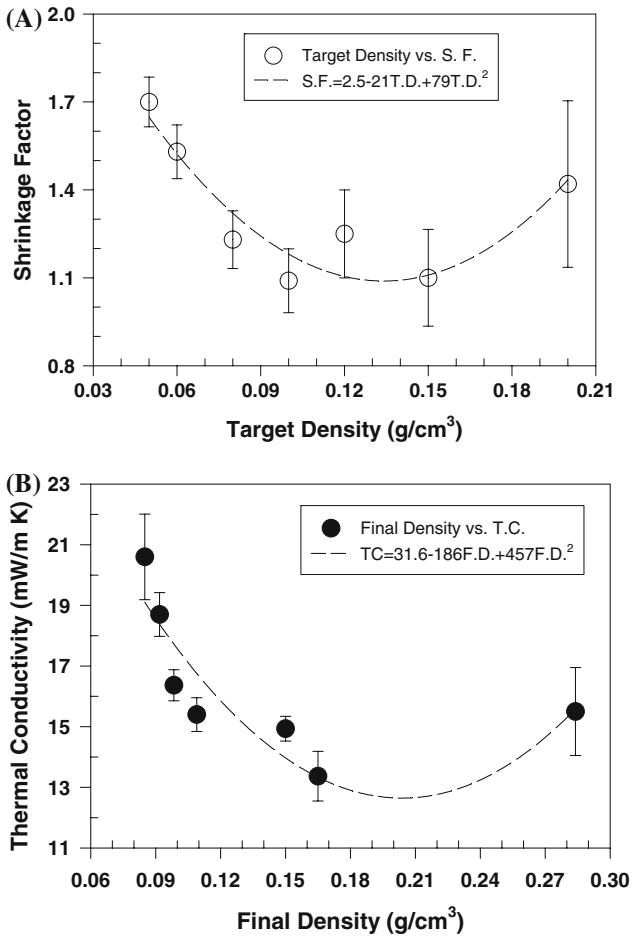

Fig. 6 The effect of target and final density on shrinkage factor (**a**) and thermal conductivity values at ambient condition (**b**), respectively, of the resultant polyurea based aerogels prepared with a constant EW ratio of 0.1 and a catalyst content of 5 wt%

Our current results observed from polyurea based aerogel are consistent with those of Lu et al. [20] and Hümmer et al. [32] that demonstrated the minimum thermal conductivity for their organic resorcinol-formaldehyde based aerogel and the opacified silica based aerogel powders at a certain density. Based on Hümmer et al.'s study [32], lower total thermal conductivity values as the density increases may occur due to the decreasing gas conduction and radiation heat transfer contributions which outweigh the increasing solid thermal conductivity contribution due to the higher densities. However, as the density increases further, the conductivity of the solid increases further and clearly becomes the dominant heat conduction mechanism, and consequently, the total thermal conductivity values of materials increase. A more detailed description of the relationship between the thermal conductivity value of aerogels and heat transfer mechanisms such as solid conduction, gaseous conduction, and radiation conduction as a function of the final density can be found in [32].

Figure 6 shows that our polyurea aerogel shows the minimum thermal conductivity value at the final density around 0.20 g/cm^3. Lu et al. [20] showed the lowest thermal conductivity values of the resorcinol-formaldehyde aerogel at density of around 0.16 g/cm^3 in air, while Lee and Gould [28] also reported the lowest thermal conductivity values of pDCPD based aerogel at density of around 0.21 g/cm^3. On the other hand, Hümmer et al. [32] observed the minimum total thermal conductivity values of the opacified silica based aerogel powders at density of around 0.12 g/cm^3. The specific final densities for the minimum thermal conductivity of the different types of aerogels may be associated with material solid conductivities, and aerogel pore size and morphology. Also, Fig. 6 shows that the minimum thermal conductivity values of about 13 mW/m K for the polyurea based aerogels are comparable with those of resorcinol-formaldehyde based aerogel monolith (12 mW/m K) [20] and opacified silica based aerogel (13 mW/m K) [32] and are lower than those of pDCPD based aerogels (16 mW/m K) [28] and PU based aerogels (22 mW/m K) [27].

To determine the optimum target density and EW ratio, a DOE experiment was conducted with narrow variable levels using 5 and 10 wt% catalyst content as shown in Table 3. Since similar results were obtained from samples prepared with 5 and 10 wt% catalyst, the results obtained from samples prepared with the catalyst content of 5 wt% were used to examine properties in more detail. The effects of target density and EW ratio on gel time, total porosity calculated from the final density (i.e., shrinkage factor), and thermal conductivity values measured at room

Table 5 Gel time, porosity, and thermal conductivity values of polyurea 2 based aerogel samples prepared with a catalyst content of 5 wt% compared with predictions calculated by DOE program

Exp. No.	Gel time (min)	Prediction by DOE	Porosity[a] (%)	Prediction by DOE	Thermal conductivity (mW/m K)	Prediction by DOE
DOE-1	34	49	93.8	94.1	18.0 ± 1.6	17.8
DOE-2	44	53	94.1	93.8	17.9 ± 0.7	18.3
DOE-3	98	74	91.8	91.8	17.2 ± 1.5	17.0
DOE-4	29	22	91.8	91.8	15.5 ± 1.0	15.7
DOE-5	31	26	91.5	91.4	15.9 ± 1.8	16.2
DOE-6	35	47	89.3	89.4	15.4 ± 1.1	14.9
DOE-7	21	13	91.6	91.3	15.2 ± 1.3	15.2
DOE-8	23	18	90.6	91.0	16.5 ± 0.9	15.8
DOE-9	26	38	89.0	88.9	13.7 ± 0.8	14.4

[a] Porosity (%) of samples = 100 − [[polyurea aerogel density/material (polyurea) density g/cm^3] × 100]. We assumed 1.20 g/cm^3 as a material density based on densities of pMDI and polyamine and the average weight ratio used for this study

temperature (37.8 °C) of polyurea prepared with the catalyst content of 5 wt% are numerically analyzed and the results summarized in Table 5.

The data listed in Table 5 shows that the experimental and predicted porosity and thermal conductivity values by DOE software are quite consistent, while a slight difference is observed from the experimental and predicted gel time, especially for samples prepared with lower target density. On the other hand, the irregular shrinkage and the resulting changes to pore structure appear to be affected by processing variables such as mixing intensity and time, aging period and temperature, and supercritical drying conditions. Slight variations in these factors may be responsible for the discrepancies observed between experimental and DOE predictions for these samples.

The data listed in Table 5 shows that target density and EW ratio play important roles in determining the gel time and the total porosity of the polyurea aerogels, while the thermal conductivity values are not significantly affected by EW ratio. As target density and EW ratio increase, faster gel time, lower total porosity, and lower thermal conductivity values are observed for the polyurea based aerogels. The effects of target density on the gel time and thermal conductivity values of the polyurea based aerogels are very consistent with previous results shown in Figs. 5 and 6. The relationships between material variables and gel time, the porosity, and thermal conductivity value obtained are indicated by Eq. 3–5, respectively:

$$\text{Gel Time (min)} = 253 - 4617X_1 - 377X_2 + 23333X_1^2 + 3133X_2^2 \quad (3)$$

$$\text{Porosity}(\%) = 111 - 451X_1 + 44X_2 + 2395X_1^2 - 340X_2^2 \quad (4)$$

$$\text{Thermal Conductivity (mW/m K)} = 31 - 383X_1 + 68X_2 + 1992X_1^2 - 381X_2^2 \quad (5)$$

where X_1 and X_2 are target density and EW ratios of polyamine hardener to isocyanate, respectively. The gel time, porosity, and thermal conductivity predicted with Eqs. 3–5 are included in Table 5 with experimental results, as discussed earlier. More detailed discussion of the DOE method can be found in [28].

Figure 7 illustrates the relationships between the target density, EW ratio and the thermal conductivity of the polyurea aerogel prepared using 5% and 10% catalyst content along with the best regression planes. The regression planes are mainly included as an aid to guide the reader's eye and indicate that samples prepared with lower catalyst content of 5 wt% have lower thermal conductivity values than those of samples prepared with higher catalyst content of 10 wt%. Also, as discussed earlier, Fig. 7

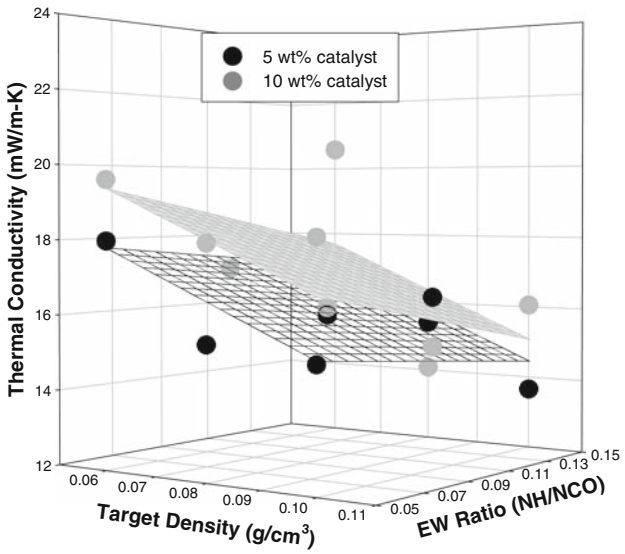

Fig. 7 The effect of catalyst content, target density, and EW ratio on the thermal conductivity values of polyurea based aerogel monoliths along with the best regression planes

demonstrates that target density plays a predominant role in determining the thermal conductivity values of the polyurea based aerogels. This result is not consistent with previous results shown in Table 2 and Fig. 3 in that EW ratio significantly affected the shrinkage factor and thermal conductivity of the polyurea based aerogels prepared with the wide range of EW ratios. The levels of EW ratios used for this DOE study are probably close to the optimum values to obtain low thermal conductivities for the polyurea based aerogels.

Figure 8 illustrates the thermal conductivity of polyurea and PU based aerogels at pressures from 0.075 torr to ambient pressure of 760 torr. Table 6 provides the numerical thermal conductivity values at 0.075 and 760 torr of polyurea based aerogel samples as well as their target and final densities and the total porosities. The differences in thermal conductivity values obtained between 0.075 and 760 torr may be associated with the gas conduction [33] or air filled effect [24] which is not a factor at low pressures. Since the gas conduction contribution is eliminated under vacuum, the thermal conductivity values at 0.075 torr are determined by the characteristic material solid conductivity [20, 33]. The gas conduction of aerogel products is closely related to the pore volume, surface area, size and the pore size distribution. Additional discussion on detailed pore structures and morphologies of polyurea based aerogel samples will be provided later.

Figure 8 and Table 6 indicate that high density polyurea 1 and 2 based aerogel samples exhibit similar or slightly lower thermal conductivities at high pressure relative to ambient pressure, while low density polyurea 1 and 2 based aerogels exhibit the lower thermal conductivities at low pressure. Consequently, high density samples have higher thermal conductivity values at low pressure than those of low density samples. Thermal conductivity of PU based aerogels as a function of pressure is similar to those of polyurea based aerogels.

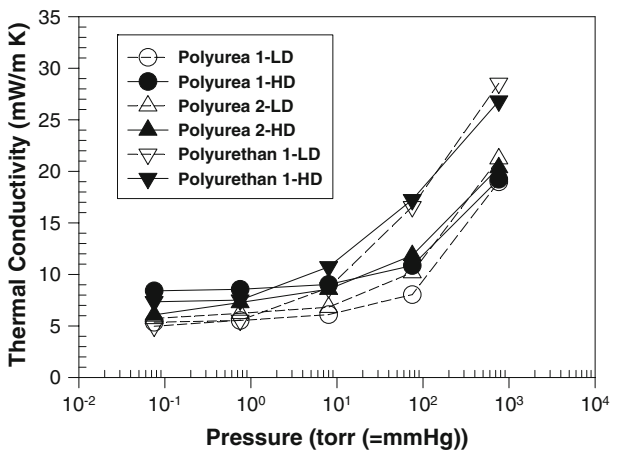

Fig. 8 Thermal conductivity of polyurea 1 and 2 and PU based aerogels prepared with target densities of 0.07 (LD) and 0.1 g/cm^3 (HD) as a function of pressure

These thermal conductivity behaviors observed from polyurea and PU based aerogels as a function of different pressure are consistent with the previous results of Lu et al. [20]. Decreasing thermal conductivity values of polyurea and PU based aerogels at decreasing pressures is closely associated with decreasing gas conduction [33]. Also, their better thermal conductivity values at relatively low pressure may occur due to their lower solid conductivity [20, 33]. As a result, the low density polyurea 1 and 2 aerogels demonstrated better thermal conductivity values at low pressures than those of their high density samples.

Figure 9 shows a plot of thermal conductivity of the low density polyurea 2 aerogel sample measured under a low vacuum pressure of 8 torr as a function of temperature. Figure 9 shows that the thermal conductivity value of the polyurea aerogel sample decreases linearly with decreasing temperature under the pressure of 8 torr demonstrating thermal conductivity values between 2.0 and 5.7 mW/m K. The decreasing thermal conductivity values of the polyurea aerogel sample with decreasing temperature may be associated with decreasing radiation heat transfer as the temperature decreases. Scheuerpflug et al. [34] demonstrated with the silica based aerogel sample that the radiation effect rapidly increases with increasing temperature so that the radiation effect represents less than 5% of the solid conduction heat transfer at 40 K, is equal to the solid conductivity at approximately 240 K, and become about 2.5 times that of solid conductivity at 300 K.

The thermal conductivity values of aerogels are affected by the pore volume, surface area, and the average pore size. Table 7 provides the final densities, pore volumes, average sizes, surface areas, and thermal conductivity values of two polyurea, PU, and silica based aerogel monolith samples. A relatively low degassing temperature of 70 °C was used for BET and pore size analysis of organic polyurea and PU based aerogels, while a degassing temperature of 105 °C was used for analysis of silica based aerogels (see Sect. 2). The data listed in Table 7 shows that the silica aerogel has the highest BET pore volume and surface area, followed by polyurea 1 and 2 based aerogels, while PU based aerogels exhibited the least nanopore volume and surface area. The lowest and highest thermal conductivity values exhibited by silica and PU based aerogels, respectively, are likely associated with the differences in their pore volumes and surface areas. The pore volume and surface area observed from our PU aerogel are very consistent with those determined by Rigacci et al. [27]. On the other hand, polyurea 1 and polyurea 2 based aerogels with similar densities demonstrate comparable thermal conductivity values and surface areas. As observed from the data in Table 7, polyurea 1 based aerogels contained almost 1.7 times the

Table 6 Densities, porosities, and thermal conductivity values at 760 and 0.075 torr for the polyurea and PU aerogels

Samples[a]	Target density (g/cm^3)	Final density (g/cm^3)	Porosity (%)	T.C. (mW/m K)	
				760 torr	0.075 torr
Polyurea 1-LD	0.07	0.0986	91.8	18.97	5.35
Polyurea 1-HD	0.1	0.1182	90.2	19.22	8.40
Polyurea 2-LD	0.07	0.1073	91.1	21.22	5.73
Polyurea 2-HD	0.1	0.1163	90.3	20.37	6.08
PU 1-LD	0.07	0.0956	92.0	28.53	4.97
PU 1-HD	0.1	0.1152	90.4	26.81	7.35

[a] Aerogel samples were prepared with a constant catalyst content of 5 wt% and a EW ratio of 1.0

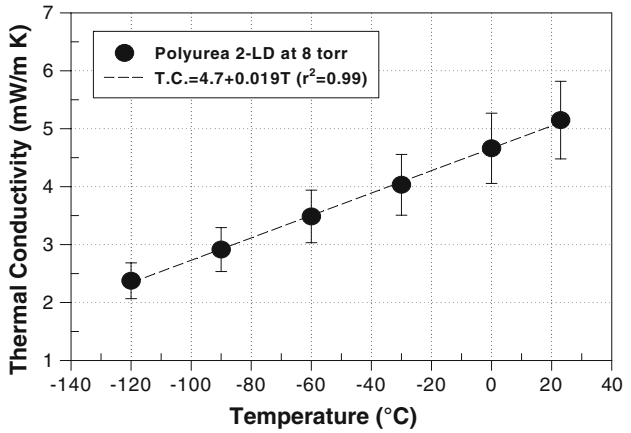

Fig. 9 Thermal conductivity of the polyurea 2 based aerogel as a function of temperature under a pressure of 8 torr

pore volume of polyurea 2 based aerogel, while smaller pores are included in polyurea 2 based aerogel as indicated by smaller average pore diameter. As a result, the average sizes of pores in aerogel materials also play an important role in determining their thermal conductivity values.

Figure 10 illustrates the pore size distributions of polyurea 1 and 2 and PU based aerogel monoliths and the adsorption and desorption isotherms for a polyurea 2 based aerogel. Figure 10a shows that polyurea based aerogels have wider pore size distributions than the PU aerogel. As discussed before, polyurea 2 aerogel contains a higher volume of smaller pores (less than 10 nm) than polyurea 1 and PU based aerogels.

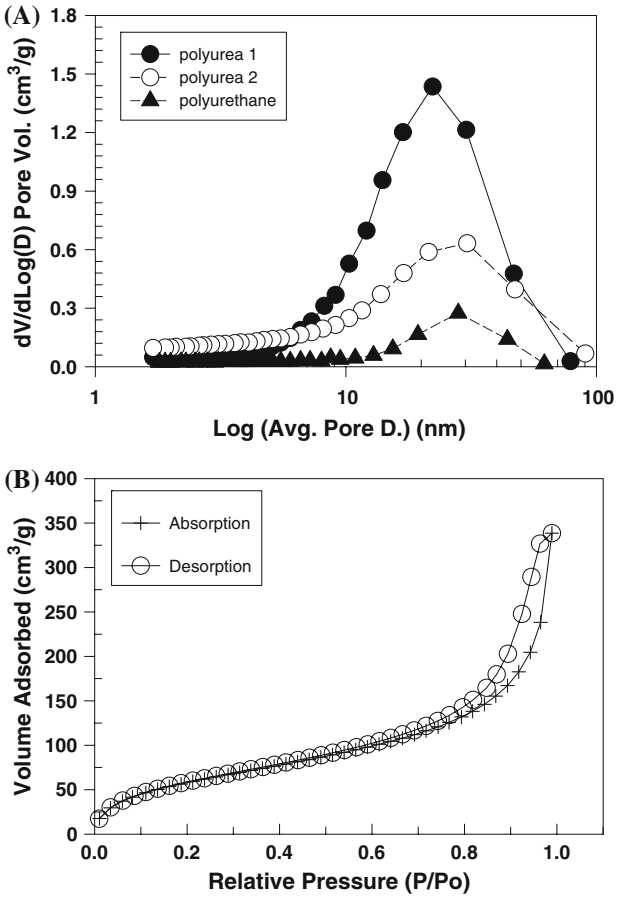

Fig. 10 Pore size distributions of polyurea 1 and 2 and PU based aerogels (**a**) and the adsorption and desorption isotherm for a polyurea 2 based aerogel (**b**)

Table 7 Densities, nanopore volumes, average sizes, surface areas, and thermal conductivity values of polyurea, PU, and silica based aerogels

Samples	Density (g/cc)	Pore volume (cm^3/g)	Average pore diameter (nm)	Surface area (m^2/g)	Thermal conductivity (mW/m K)
Polyurea 1[a]	0.1182	0.91	19	189	18.2
Polyurea 2[a]	0.1163	0.58	12	192	19.2
PU[a]	0.1277	0.16	13.0	47	27.0
Silica[b]	0.0902	2.86	13.7	686	12.0

[a] Degassing at temperature of 70 °C for 12 h under the vacuum

[b] Degassing at temperature of 105 °C for 12 h under the vacuum

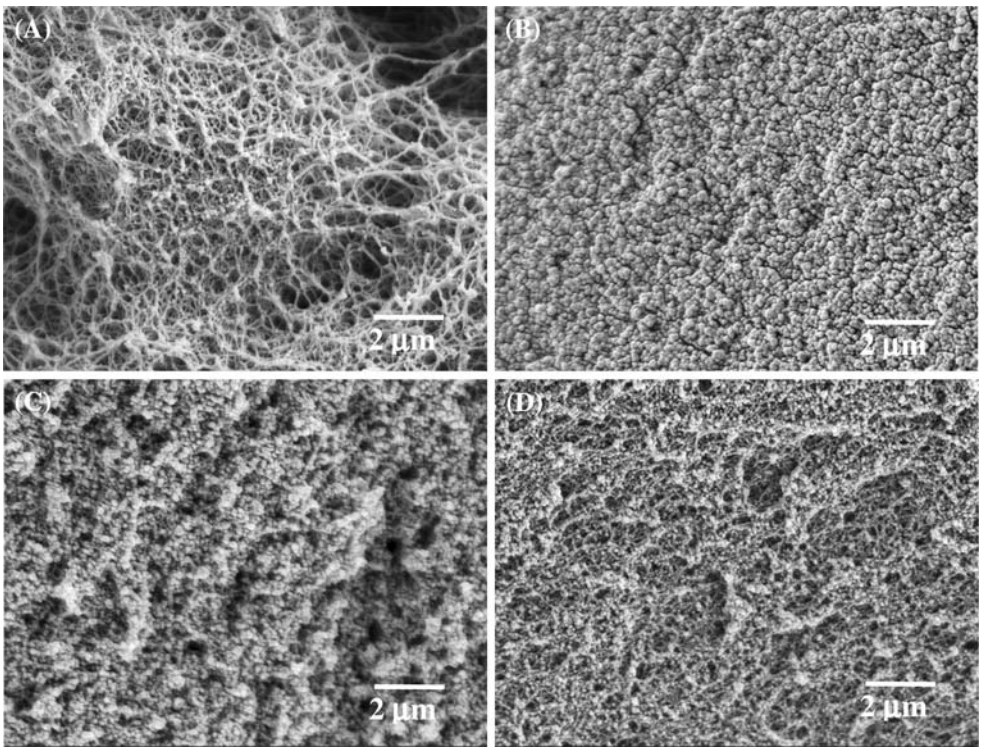

Fig. 11 SEMs of PU (**a**), silica (**b**) and polyurea based aerogels of Exp-2 (**c**) and Exp-4 (**d**) prepared with two different target densities of 0.06 and 0.1 g/cm^3, respectively, measured at magnification of X10 K

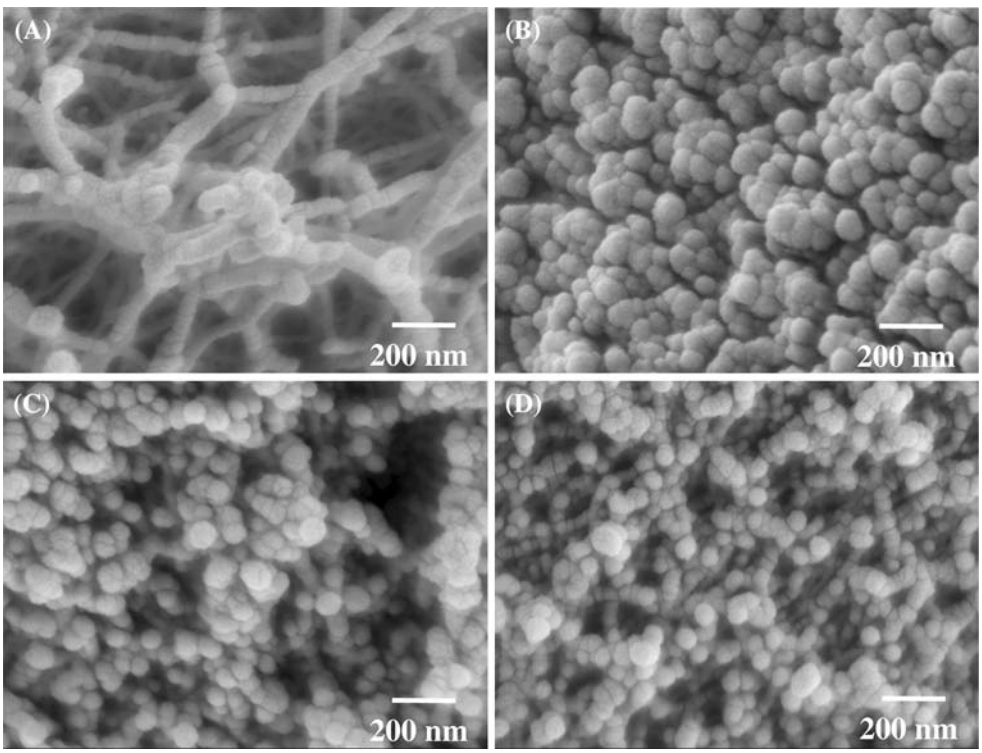

Fig. 12 SEMs of PU (**a**), silica (**b**) and polyurea based aerogels of Exp-2 (**c**) and Exp-4 (**d**) prepared with two different target densities of 0.06 and 0.1 g/cm^3 measured at magnification of X60 K

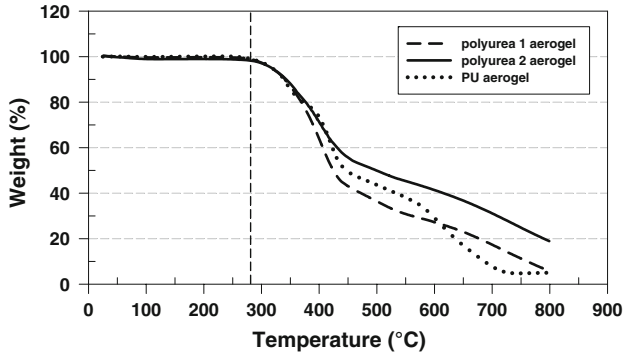

Fig. 13 TGAs of polyurea 1, polyurea 2, and PU based aerogels prepared with target density of 0.1 g/cm^3

Figure 11 shows the SEM photos and illustrates the microstructures of PU, silica, and polyurea based aerogels with two different densities of 0.06 and 0.1 g/cm^3 (Exp-2 and Exp-4, see Table 2) measured at magnifications of X10 K. The SEMs obtained at magnifications of X60 K are shown in Figure 12. Figures 11 and 12 show that silica based aerogel contains the least pores and consists of ~50 nm clusters of nanosized silica particles. The polyurea aerogels have similar microstructures, and the high density polyurea based aerogel has larger pores than the silica aerogel. The low density polyurea contains some macropores, while the PU based aerogels exhibit a fibrillar morphology containing macrosized (>100 nm) pores. The large pores (possibly defects) observed by SEM in PU and low density polyurea based aerogels may increase their gaseous and radiation thermal conductivity contributions [33] resulting in higher thermal conductivities. In order to significantly improve the thermal conductivity performances of polyurea based aerogels, especially low density polyurea aerogels, further optimization of processing methods will be required focusing on the relationship between large pores and processing conditions.

Figure 13 demonstrates the mass loss of polyurea 1 and 2 and PU based aerogels measured by thermogravimetric analysis (TGA) in air. The initial mass loss is low indicating that outgassing of volatile materials at low temperature is minimal which is important for spacecraft and spacesuit insulation applications. The TGA illustrated in Fig. 13 shows that polyurea 1 and 2 and PU based aerogel samples are relatively stable up to 270 °C. Since the varying thermal stability may be associated with the structures of the aerogel materials, the higher thermal stability of polyurea 2 based aerogel may be due to a more thermally stable structure formed by using a polymeric isocyanate (pMDI) instead of the monomeric MDI.

4 Conclusion

In this study we demonstrated that lightweight nanoporous polyurea based aerogels can be produced by using a simple sol–gel processing and supercritical drying method and investigated their physical and thermal properties and pore sizes. The uniform polyurea gels were formed from the reaction between isocyanate precursors and polyamine hardeners at room temperature and atmospheric pressure. Supercritical CO_2 drying method was successfully used to produce polyurea aerogels from their wet gels. The polyurea based aerogel exhibited a wide range of final densities and had little dustiness, high porosity (including mesoporosity), low shrinkage, low thermal conductivities, good hydrophobicity, and high thermal stability. Both target density and equivalent weight ratio between isocyanate resin and polyamine hardener played very important roles in determining sample appearance, shrinkage factor, and thermal conductivity values of the polyurea aerogels. We also found that the polyurea based aerogel contained higher pore volume and surface areas and smaller pore sizes than the PU aerogel, which is a main reason the polyurea aerogels exhibit good thermal conductivity values at a wide range of pressures and temperatures. The polyurea aerogels are very promising candidates for many thermal insulation applications including spacesuit insulation.

Acknowledgment This work was conducted by the financial support of the United States National Aeronautics and Space Administration (NASA), SBIR Contract No. NNJ04JA22C. The authors are grateful to Mr. Max Mesham, Ms. Geeta Bhakhari, and Mr. Nathan Bhobho for their helps in preparing samples and also, to Ms. Sara Rosenberg, Dr. Jenifer Marchesi, and Dr. Shannon White for their valuable helps. The authors would like to thank Ms. Evelyn S. Orndoff and Mr. Luis A. Trevino of NASA for their continuous supports for this work. The authors are also grateful to TPRL for thermal conductivity measurement at different pressures and temperatures and Dow Corning Analytical Lab for SEM measurement.

References

1. Kistler SS (1931) Nature 127:741. doi:10.1038/127741a0
2. Kistler SS (1932) J Phys Chem 36:52. doi:10.1021/j150331a003
3. Hüsing N, Schubert U (1998) Angew Chem Int Ed 37:22
4. Pierre AC, Pajonk GM (2002) Chem Rev 102:4243. doi:10.1021/cr0101306
5. Pajonk GM (2003) Colloid Polym Sci 281:637. doi:10.1007/s00396-002-0814-9
6. Bisson A, Rigacci A, Lecomte D, Rodier E, Achard P (2003) Dry Technol 21:593. doi:10.1081/DRT-120019055
7. Akimov YK (2003) Instrum Exp Tech 46:287. doi:10.1023/A:1024401803057
8. LeMay JD, Hopper RW, Hrubesh LW, Pekala RW (1990) MRS Bull 15(12):19
9. Schaefer D (1994) MRS Bull 19(4):49
10. Hrubesh LW, Poco JF (1995) J Non-Cryst Solids 188:46. doi:10.1016/0022-3093(95)00028-3

11. Schmidt M, Schwertfeger F (1998) J Non-Cryst Solids 225:364. doi:10.1016/S0022-3093(98)00054-4
12. Fricke J, Emmerling A (1998) J Sol–Gel Sci Technol (Paris) 13:299
13. www.aerogel.com
14. Pekala RW, Schaefer DW (1993) Macromolecules 26:5487. doi:10.1021/ma00072a029
15. Pekala RW (1989) J Mater Sci 24:3221. doi:10.1007/BF01139044
16. Pekala RW, Kong FM (1989) Polymer Prepr 30:221
17. Ward RL, Pekala RW (1990) Polymer Prepr 31:167
18. Pekala RW, Alviso CT, LeMay JD (1990) J Non-Cryst Solids 125:67. doi:10.1016/0022-3093(90)90324-F
19. Pekala RW, Alviso CT, Kong FM, Hulsey SS (1992) J Non-Cryst Solids 145:90. doi:10.1016/S0022-3093(05)80436-3
20. Lu X, Arduini-Schuster MC, Kuhn J, Nilsson O, Fricke J, Pekala RW (1992) Science 255:971. doi:10.1126/science.255.5047.971
21. Lu X, Caps R, Fricke J, Alviso CT, Pekala RW (1995) J Non-Cryst Solids 188:226. doi:10.1016/0022-3093(95)00191-3
22. Tan C, Fung BM, Newman JK, Vu C (2001) Adv Mater 13:644. doi:10.1002/1521-4095(200105)13:9<644::AID-ADMA644>3.0.CO;2-#
23. Fischer F, Rigarcci A, Pirad R, Berthon-Fabry S, Achard P (2006) Polymer (Guildf) 47:7636. doi:10.1016/j.polymer.2006.09.004
24. Biesmans G, Randall D, Francais E, Perrut M (1998) J Non-Cryst Solids 225:36. doi:10.1016/S0022-3093(98)00103-3
25. Biesmans G, Mertens A, Duffours L, Woignier T, Phalippou J (1998) J Non-Cryst Solids 225:64. doi:10.1016/S0022-3093(98)00010-6
26. Lee JK, Shannon W, Mesham M, Gould GL (2006) NASA SBIR Phase II Contract No. NNJ04JA22C Final Report, March
27. Rigacci A, Marechal JC, Repoux M, Moreno M, Achard P (2004) J Non-Cryst Solids 350:372. doi:10.1016/j.jnoncrysol.2004.06.049
28. Lee JK, Gould GL (2007) J Sol–Gel Sci Technol (Paris) 44:29
29. Kramer DP, McNeil DC, Howell EI, Gembarovic J, Taylor RE (2002) Proceedings of the 37th intersociety energy conversion engineering conference (IECEC), IEEE, Catalog #02CH37298, July 2002, paper 20089
30. Bittle RR, Taylor RE (1984) J Am Ceram Soc 67:186
31. Lee JK, Gould GL (2005) J Sol–Gel Sci Technol (Paris) 34:281
32. Hummer E, Rettelbach T, Lu X, Fricke J (1993) Thermochim Acta 218:269. doi:10.1016/0040-6031(93)80428-D
33. Lee OJ, Lee KH, Kim SY, Yoo KP (2002) J Non-Cryst Solids 298:287. doi:10.1016/S0022-3093(01)01041-9
34. Scheuerpflug P, Morper HJ, Neubert G, Fricke J (1991) J Phys D Appl Phys 24:1395. doi:10.1088/0022-3727/24/8/025